COMMUNICATION

Check for updates

Facile one-pot synthesis of γ-Fe₂O₃ nanoparticles by inductive heating

Pratikshya Sharma, [ID] [a] Peter Heinz Pfromm, [bc] Bin Liu [b] and Viktor Chikan [ID] *[a]

The direct one-pot synthesis of γ-Fe₂O₃ nanoparticles (NPs) has been demonstrated through a facile inductive heating method. Acetylferrocene, a solid precursor, has been used for the first time to the best of our knowledge during the synthesis. Traditionally, solid precursors have not been used in the hot-injection (HI) technique because of their limited solubility and less likely outcome to produce the high supersaturation needed for diffusion-limited growth of the NPs. Oleylamine and trioctylamine serve as a solvent, a binding ligand, and a reducing agent in the synthesis to produce γ-Fe₂O₃ NPs with relatively narrow size distribution. The structures, morphologies, and magnetic properties of γ-Fe₂O₃ NPs are studied. The phase pure γ-Fe₂O₃ NPs obtained display uniform morphology and good magnetic property. Therefore, the inductive heating technique has the potential to provide an industrial level scale-up synthesis in continuous reactors, which is not available for the HI method relying on batch synthesis.

1. Introduction

Colloidal magnetic nanoparticles such as iron oxide nanoparticles (IONPs) are very fascinating due to their usefulness in various fields such as biomedical and chemical engineering.[1–4] Particularly, γ-Fe₂O₃ NPs are more attractive due to their distinct properties like stability, biocompatibility, superparamagnetism, low Curie temperature, and high magnetic susceptibility.[3,5–10] Because of these unique properties, γ-Fe₂O₃ NPs are used in magnetic resonance imaging (MRI) contrast enhancement, bio-magnetic separation, hyperthermia treatment and magnetic drug targeting, multi-terabyte storage, catalysis, biosensors, bio-separation, and thermoablation.[11–18] The most common method to synthesize colloidal γ-Fe₂O₃ NPs is

the HI method.[19,20] In this technique, small amounts of precursor molecules are injected into a hot boiling solvent, which results in rapid decomposition of the molecular precursors thus producing inorganic nanomaterials (oxides, and semiconductors).[20–24]

While the HI method for colloidal synthesis is very well-established and useful, there are drawbacks to this methodology.[22,25,26] The rapid injection of the precursor might produce uneven nucleation due to the limited heat and mass transport of the molecules during the application of the HI process in typical batch reactors.[22] In addition, precursor molecules are usually miscible liquids that can ensure high concentration in the solution after injection causing solid precursors to have limited use in the HI method due to solubility limits.[22,25] Furthermore, scaling up in the hot-injection method designed for laboratory scale synthesis is difficult due to low yield and non-uniform heat transport.[22]

There are many examples reported in the literature regarding the use of the HI method to prepare IONPs. For instance, Hyeon et al. showed the non-hydrolytic method to produce monodisperse and highly crystalline γ-Fe₂O₃. The resulting NPs were of size ranging from the 4–16 nm diameter.[27] However, these synthetic protocols are complex, requiring a mixture of multiple solvents (octyl ether and oleic acid) and a long heating time followed by refluxing. In addition to this, Das and et.al. reported the solventless synthesis of IONPs through thermal decomposition of acetylferrocene.[28] In their work they used malic anhydride as a co-precursor. The resulting nanoparticle size ranged from 10–20 nm. However, their approach requires a precursor to be heated in a furnace at a higher temperature and longer reaction time i.e., 1300 K for 4 hours resulting in irregularly shaped NPs. While on the other hand, inductive heating (IH) synthesis of nanomaterials provides high heating rates (100–300 °C s⁻¹) to produce a similar result as for HI methods.[22,25] The method consist of an induction heating reactor with steel balls placed inside. The reactor stays within an induction coil that rapidly heats the steel balls producing boiling solvent and decomposition of precursor molecules. In this technique, the heating medium located inside of the

[a] Department of Chemistry, College of Arts and Sciences, Kansas State University, Manhattan, KS 66506, USA. E-mail: vchikan@ksu.edu

[b] Department of Chemical Engineering, Carl R. Ice College of Engineering, Kansas State University, Manhattan, KS 66506, USA

[c] The Gene and Linda Voiland School of Chemical Engineering and Bioengineering, Washington State University, Pullman, WA 99164-6515, USA

reactor, the contact surface area with the solvent is very large. The heating of the actual reaction vessel is not necessary to reach the decomposition temperature of the precursor molecules required for fast heating rates. We have recently shown that the use of steel balls provides a strongly reducing environment, therefore, removing any trace level of oxygen in typical nanomaterials making it possible to synthesize the reduced state of metal NPs.[29]

Our research group has successfully developed the IH method for the synthesis of monodisperse, air-stable iron, iron oxide NPs, and CdSe quantum dots in past years.[25,29] In the recent work, our group has been able to prepare air-stable iron and IONPs (β-Fe$_2$O$_3$, γ-Fe$_2$O$_3$, and Fe$_3$O$_4$ NPs) with controlled size *via* the IH technique.[29] On further extending that work, herein we explore the use of IH synthesis of phase pure γ-Fe$_2$O$_3$ NPs from a solid precursor, acetylferrocene which avoids the use of toxic and expensive organometallic compounds like iron pentacarbonyl precursor. To the best of our knowledge, the use of solid precursors for the preparation of IONPs *via* IH has not

been reported. The motivation for this work comes from the need for rapid single-step, one-pot synthesis of monodisperse and uniform colloidal γ-Fe$_2$O$_3$ NPs using a solid precursor, therefore extending the range of precursors that can be used in NP synthesis. Herein, we demonstrate a direct one-pot method to synthesize γ-Fe$_2$O$_3$ NPs within a few seconds *via* the IH technique using acetylferrocene as a solid precursor. The size, magnetic behavior, and crystallinity of the synthesized IONPs using a solid precursor (acetylferrocene) and different solvents (oleylamine and trioctylamine) at different reaction times are studied. The resulting NPs were γ-Fe$_2$O$_3$ NPs confirmed by high-resolution transmission electron microscopy (HRTEM) and powder X-ray diffraction (PXRD) patterns.

2. Result and discussion

The synthesis method and IH reactor experimental setup was based on literature with some modifications.[22,25,29,30] For a typical
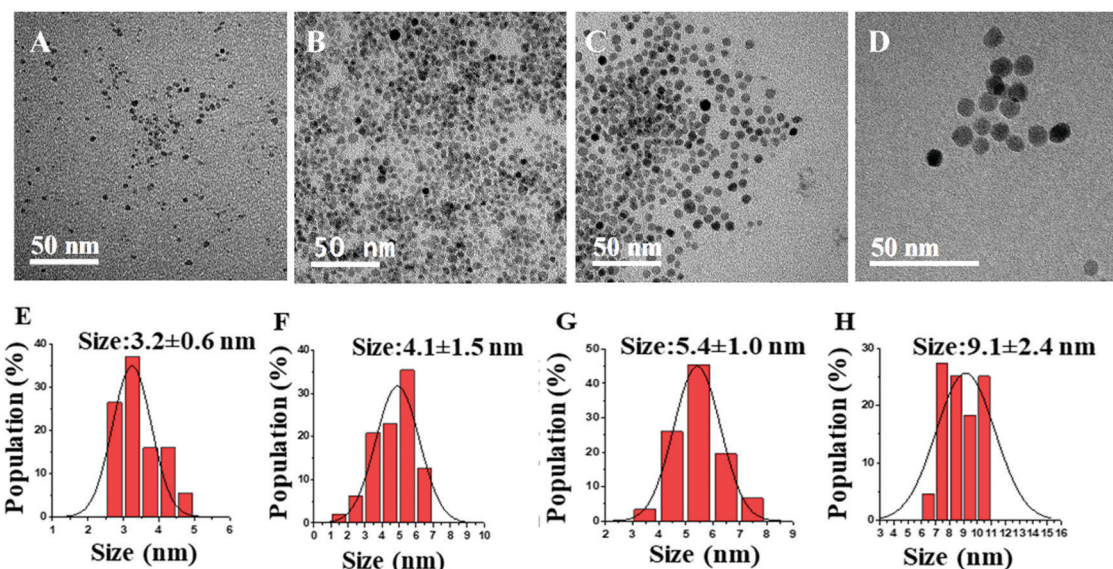

Fig. 1 TEM images of γ-Fe$_2$O$_3$ NPs produced by using 0.8 M acetylferrocene and oleylamine at different reaction times (A) 5 s, (B) 7 s, (C) 10 s, and (D) 14 s. (E–H) are the particle size distribution plots, respectively.
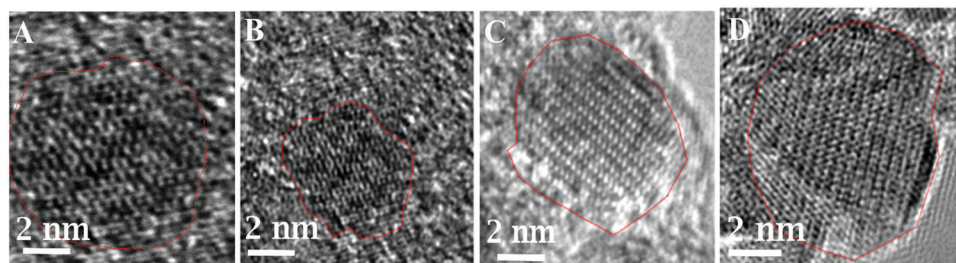

Fig. 2 HRTEM images of γ-Fe$_2$O$_3$ NPs produced by using 0.8 M acetylferrocene, and oleylamine at different reaction times (A) 5 s, (B) 7 s, (C) 10 s, and (D) 14 s. (A) indicates (222) lattice plane, (B) indicates (026), (222) lattice planes, (C) indicates (111), (123), (026) lattice planes, and (D) indicates (112), (222), (017) lattice planes of γ-Fe$_2$O$_3$ NPs.
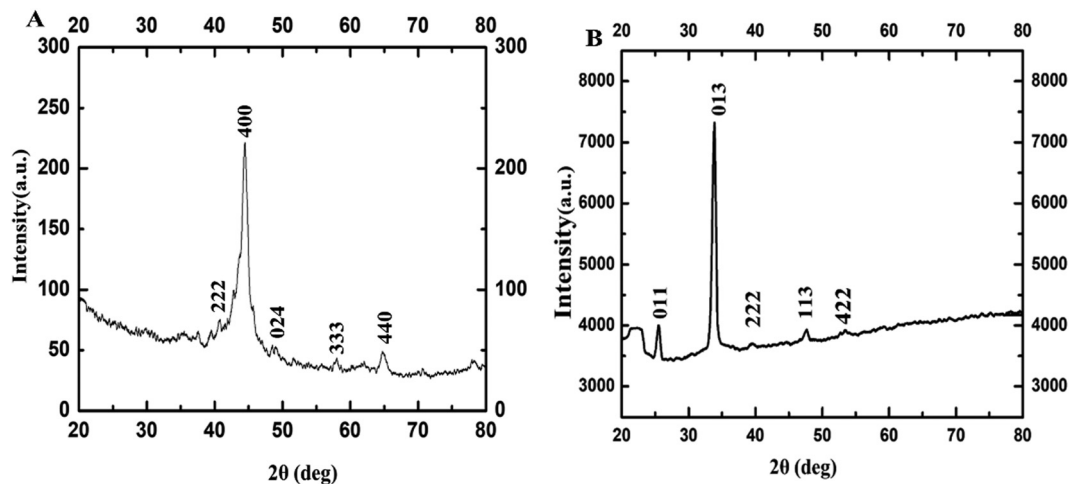
Fig. 3   PXRD of γ-Fe_2O_3 NPs synthesized using 0.8 M acetylferrocene and oleylamine at (A) 10 s, and (B) 14 s heating.

synthesis, the stock solution was prepared by stirring the mixture of acetylferrocene with the solvent (0.8 M) for 24 hours. Then, the reactor was filled with steel balls (25.92 g, Bearing-Quality E52100 Alloy Steel, Hardened Ball, 1/8″ diameter) and transported to a nitrogen-filled glovebox. Next, 4 mL precursor solution was transferred from the stock solution to the reactor. Following this, the reactor was inserted into the coil of the inductive heater (standard 10 kW inductive heater) and connected to tubing which maintains an argon atmosphere throughout the reaction. Then, the reaction mixture was heated in a set at minimum power for 5 s, 7 s, 10 s, and 14 s to control the size, crystallinity, and magnetic behavior of synthesized IONPs using varying reaction times, solvents. The reddish solution turns darker black with increasing reaction time indicating the formation of IONPs. The synthesized NP solution was cooled to room temperature, then isolated by centrifuging using methanol ($\sim$20–25 mL) at 8000 rpm for 10 minutes followed by sonication. This process was repeated three times. The colorless supernatant was discarded, and the precipitated NPs were then dispersed in small quantities of toluene (3–4 mL) for glovebox storage until further use.

The γ-Fe_2O_3 NPs were synthesized with a single solid precursor (acetylferrocene) and two different solvents (oleylamine and trioctylamine) at various reaction times. The comparative study on the size, crystallinity, and magnetization of IONPs with the change in reaction time and boiling point of solvent is demonstrated. The morphology and structure of the pure γ-Fe_2O_3 NPs are characterized by TEM. The particle size distributions, obtained from TEM micrographs, are shown in Fig. 1(A–D) and the corresponding mean particle sizes obtained from the Gaussian fit of the histograms are also indicated in Fig. 1E–H. The histogram demonstrates that as the reaction time increases the size of NPs increases. The reason behind this trend is the nucleation and growth of NPs. Longer reaction time provides more time for the growth of NPs yielding larger sizes. These particle size distribution starts to narrow as the heating time increase from 5 s to 14 s probably due to higher supersaturation as the precursor decomposes. The size of the formed

IONPs is close to that reported in the literature which discusses the solventless synthesis of IONPs through thermal decomposition of acetylferrocene and malic anhydride.[28]

The increase in the heating times from 5 s to 14 s increases the size of γ-Fe_2O_3 NPs from 3.2 $\pm$ 0.6 to 9.1 $\pm$ 2.4 nm. This is because a longer heating time promotes a faster nucleation rate resulting in larger-sized NPs. Furthermore, as the reaction time is increased, the crystallinity of the synthesized nanoparticles changed from amorphous to highly crystalline particles, as shown in HRTEM images in Fig. 2. HRTEM measurement shows the lattice spacing measurement of 2.93 (Fig. 2A), 2.95 Å, (Fig. 2B), 3.30 Å (Fig. 2C), and 3.40 Å (Fig. 2D). Fig. 2A shows (222) lattice plane, Fig. 2B shows (026), (222) lattice planes, Fig. 2C shows (111), (123), (026) lattice planes, and Fig. 2D shows (112), (222), (017) lattice planes of γ-Fe_2O_3 NPs which indicates that these particles are multidomain. These lattice planes are consistent with literature values.[29,31]
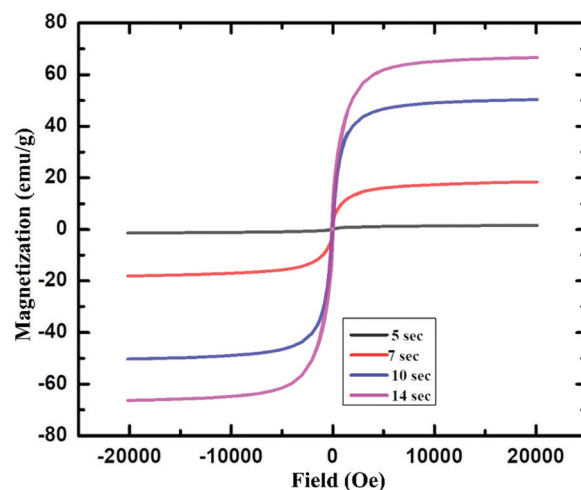

Fig. 4   Magnetization $vs.$ magnetic field plot for γ-Fe_2O_3 NPs produced using 0.8 M acetylferrocene and oleylamine 5 s, 7 s, 10 s and 14 s heating time.

This result is consistent with the lattice spacing data from the crystallography open database (COD) and density functional theory (DFT) calculations reported by Grau-Crespo *et al.*[32]

The PXRD patterns are used to determine the structural parameter of the sample. In the corresponding PXRD spectra of Fig. 3, the diffraction peaks at 2θ correspond to (011), (013), (222), (113), and (422) planes which reveal phase pure $\gamma\text{-Fe}_2\text{O}_3$ NPs with cubic crystal system (ICDD#39-1346). These values are closely in agreement with the previously reported work in literature.[32–36]

Furthermore, the magnetic property of these IONPs was studied by using a superconducting quantum interference device (SQUID). Fig. 4 shows the magnetization (emu g^{-1}) *vs.* magnetic field, H (Oe) graph for IONPs obtained by using acetylferrocene and oleylamine, at room temperature (298 K).

Fig. 4 shows that that $\gamma\text{-Fe}_2\text{O}_3$ NPs showed almost zero magnetization with heating 5 s but the saturation magnetization reaches almost 20 emu g^{-1} with the increase in heating time. The increase in M_s with an increase in size is attributed to

a decrease in a surface spin in the oleylamine surface with the increase in particle size.[37] This shows that these particles are superparamagnetic at room temperature.[29,37,38] The saturation magnetization for these particles is almost close to that of 11 nm-sized $\gamma\text{-Fe}_2\text{O}_3$ synthesized *via* thermal decomposition of $Fe(CO)_5$ as reported in the literature.[39] Furthermore, the saturation magnetization of these particles is very less as compared to that of IONPs synthesized using $Fe(CO)_5$ and atmospheric microwave plasma.[40] It can be noted from Fig. 4 that, with the increase in the size from 3.2 ± 0.6 nm to 9.1 ± 2.4 nm, the M_s value also increases from 0 to 70 emu g^{-1}. The increase in M_s value with an increase in the size of NPs could be due to the presence of magnetically disordered atoms at the surface of the NPs which is common in smaller magnetic NPs.[37,41] On the other hand, these values are less as compared to the M_s value of bulk $\gamma\text{-Fe}_2\text{O}_3$ (76 emu g^{-1}), which is probably attributed to nanoscale dimension and surface effect.[2,42,43]

Similarly, another set of experiments was performed using 0.8 M acetylferrocene and trioctylamine ($T_{bp} = 367$ °C) instead
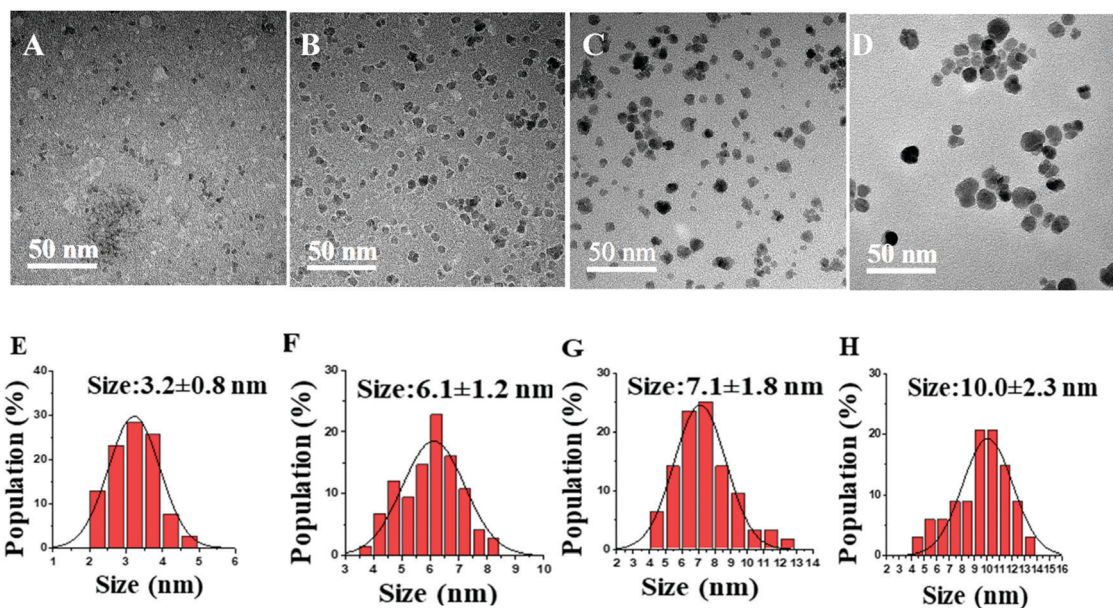

Fig. 5 TEM images of IONPs produced by using 0.8 M acetylferrocene and trioctylamine at different reaction times (A) 5 s, (B) 7 s, (C) 10 s, and (D) 14 s. (E–H) are the particle size distribution plots, respectively.
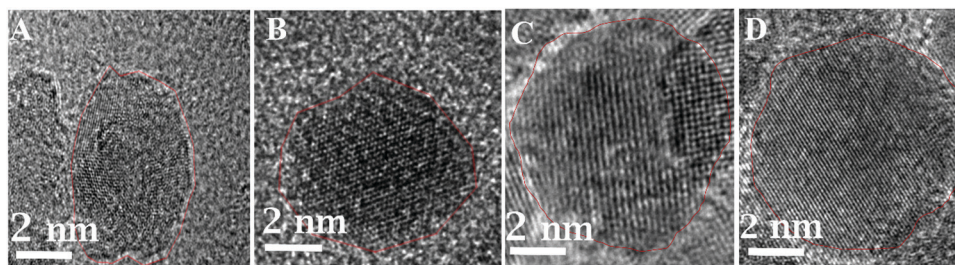

Fig. 6 HRTEM images of $\gamma\text{-Fe}_2\text{O}_3$ NPs produced by using 0.8 M acetylferrocene, and trioctylamine at different reaction times (A) 5 s, (B) 7 s, (C) 10 s and (D) 14 s. (A) indicates (222) lattice plane, (B) indicates (026), (222) lattice planes, (C) indicates (111), (123), (026) lattice planes, and (D) indicates (112), (222), (017) lattice planes of $\gamma\text{-Fe}_2\text{O}_3$ NPs.
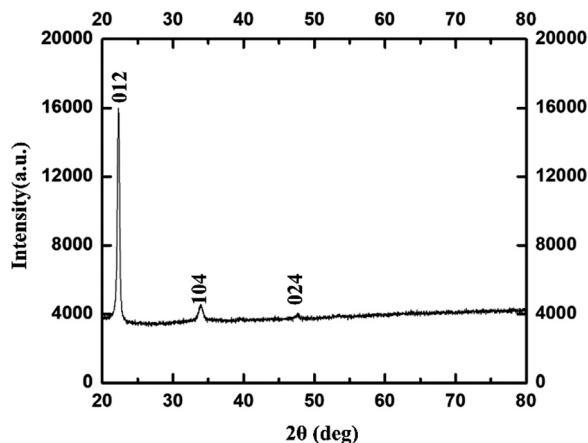
Fig. 7 PXRD of γ-Fe_2O_3 NPs synthesized using 0.8 M acetylferrocene and trioctylamine at 14 s heating.

of oleylamine (T_{bp} = 350 °C) as a solvent to see the effect of the boiling point of solvent on the size of NPs. As shown in Fig. 5, a similar trend in the size was observed with the increase in reaction time. However, the increase in size was very minimal with the increase in the boiling point of solvent under identical conditions of concentration and reaction time. Furthermore, thus synthesized nanoparticles were of very poor crystallinity as can be seen in Fig. 6 as compared to those synthesized using acetylferrocene and oleylamine (Fig. 2). To the best of our knowledge, there is not any literature report regarding the synthesis of γ-Fe_2O_3 NPs using acetylferrocene and trioctylamine; this approach could be a potential alternative way to make γ-Fe_2O_3 NPs using a single precursor and single solvent.

The HRTEM images of these nanoparticles confirm the gamma phase of Fe_2O_3. In Fig. 6, HRTEM images of these particles indicate (222), (026), (111), (123), (017), and (112) lattice planes of γ-Fe_2O_3. These values are closely in agreement with the previously reported work.[31,32]

In the corresponding PXRD spectra of Fig. 7, the diffraction peaks at 2θ correspond to (012), (104), and (024) planes which reveal phase pure γ-Fe_2O_3 NPs with cubic crystal system (ICDD#89-2810). These values are closely in agreement with the previously reported work in literature.[44]

3. Conclusion

The rapid IH approach used in this study provides a simple, facile, and inexpensive method for direct one-pot synthesis of magnetic γ-Fe_2O_3 NPs from a solid precursor. These NPs are in the size of 3–10 nm. The increase in heating times increased the size and magnetization of γ-Fe_2O_3 NPs. The result reveals that the IH method is an efficient method to produce γ-Fe_2O_3 NPs with size control and it could potentially replace the traditional HI method. We anticipate that the IH method will result in further exploration of the topic due to faster, easier, and safer preparation of various NPs and could easily be scaled up to a gram scale.

Abbreviations

NPs, nanoparticles; IONPs, iron oxide nanoparticles; TEM, transmission electron microscopy; HRTEM, high resolution transmission electron microscopy; scanning transmission electron microscopy; N_2, nitrogen; PXRD, powder X-ray diffraction, SQUID, superconducting quantum interference device.

Conflicts of interest

There are no conflicts to declare.

Acknowledgements

Notes and references

1 A. Ali, H. Zafar, M. Zia, I. Ul Haq, A. R. Phull, J. S. Ali and A. Hussain, *Nanotechnol., Sci. Appl.*, 2016, **9**, 49–67.
2 Z. Jing and S. Wu, *J. Solid State Chem.*, 2004, **177**, 1213–1218.
3 D. Cao, H. Li, L. Pan, J. Li, X. Wang, P. Jing, X. Cheng, W. Wang, J. Wang and Q. Liu, *Sci. Rep.*, 2016, **6**, 32360.
4 W. Wu, Q. He and C. Jiang, *Nanoscale Res. Lett.*, 2008, **3**, 397–415.
5 P. Wu, J. Jhu and Z. Xu, *Adv. Funct. Mater.*, 2004, **14**, 345–351.
6 M. Aslam, E. A. Schultz, T. Sun, T. Meade and V. P. Dravid, *Cryst. Growth Des.*, 2007, **7**, 471–475.
7 J. Vidal-Vidal, J. Rivas and M. A. López-Quintela, *Colloids Surf., A*, 2006, **288**, 44–51.
8 M. Abbas, Md. N. Islam, B. P. Rao, M. O. Abdel-Hamed and C. Kim, *J. Ind. Eng. Chem.*, 2015, **31**, 43–46.
9 R. Marasini, *Dissertation*, 2020, 85–106.
10 R. Marasini, T. D. Thanh Nguyen, S. Rayamajhi and S. Aryal, *Mater. Adv.*, 2020, **1**, 469–480.
11 S. I. Siddiqui, P. N. Singh, N. Tara, S. Pal, S. A. Chaudhry and I. Sinha, *Colloid Interface Sci. Commun.*, 2020, **36**, 100263.
12 M. Sharifi, S. Jafari, A. Hasan, B. A. Paray, G. Gong, Y. Zheng and M. Falahati, *ACS Biomater. Sci. Eng.*, 2020, **6**, 3574–3584.
13 M. Kamal Masud, J. Kim, M. Motasim Billah, K. Wood, M. J. A. Shiddiky, N.-T. Nguyen, R. Kumar Parsapur, Y. Valentino Kaneti, A. Ali Alshehri, Y. Gamaan Alghamidi, K. Ahmed Alzahrani, M. Adharvanachari, P. Selvam, M. S. A. Hossain and Y. Yamauchi, *J. Mater. Chem. B*, 2019, **7**, 5412–5422.
14 S. Tanaka, M. K. Masud, Y. V. Kaneti, M. J. A. Shiddiky, A. Fatehmulla, A. M. Aldhafiri, W. A. Farooq, Y. Bando, M. S. A. Hossain and Y. Yamauchi, *ChemNanoMat*, 2019, **5**, 506–513.

15 R. Marasini, T. D. T. Nguyen and S. Aryal, *Wiley Interdiscip. Rev.: Nanomed. Nanobiotechnol.*, 2020, **12**, e1580.

16 S. Cabana, A. Curcio, A. Michel, C. Wilhelm and A. Abou-Hassan, *Nanomaterials*, 2020, **10**, 1548.

17 W. Hulangamuwa, B. Acharya, V. Chikan and R. J. Rafferty, *ACS Appl. Nano Mater.*, 2020, **3**, 2414–2420.

18 B. Acharya and V. Chikan, *Magnetochemistry*, 2020, **6**, 52.

19 T. Hyeon, *Chem. Commun.*, 2003, 927–934.

20 C. B. Murray, D. J. Norris and M. G. Bawendi, *J. Am. Chem. Soc.*, 1993, **115**, 8706–8715.

21 D. A. J. Herman, P. Ferguson, S. Cheong, I. F. Hermans, B. J. Ruck, K. M. Allan, S. Prabakar, J. L. Spencer, C. D. Lendrum and R. D. Tilley, *Chem. Commun.*, 2011, **47**, 9221–9223.

22 V. Chikan and E. J. McLaurin, *Nanomaterials*, 2016, **6**, 85.

23 R. Genç, M. Ortiz and C. K. O'Sullivan, *J. Nanopart. Res.*, 2014, **16**, 2329.

24 I. S. Smolkova, N. E. Kazantseva, V. Babayan, J. Vilcakova, N. Pizurova and P. Saha, *Cryst. Growth Des.*, 2017, **17**, 2323–2332.

25 H. Luo, B. A. Kebede, E. J. McLaurin and V. Chikan, *ACS Omega*, 2018, **3**, 5399–5405.

26 J. van Embden, A. S. R. Chesman and J. J. Jasieniak, *Chem. Mater.*, 2015, **27**, 2246–2285.

27 T. Hyeon, S. S. Lee, J. Park, Y. Chung and H. B. Na, *J. Am. Chem. Soc.*, 2001, **123**, 12798–12801.

28 B. Das, J. Kusz, V. R. Reddy, M. Zubko and A. Bhattacharjee, *Solid State Sci.*, 2017, **74**, 62–69.

29 P. Sharma, N. Holliger, P. H. Pfromm, B. Liu and V. Chikan, *ACS Omega*, 2020, **5**, 19853–19860.

30 E. Muthuswamy, A. S. Iskandar, M. M. Amador and S. M. Kauzlarich, *Chem. Mater.*, 2013, **25**, 1416–1422.

31 C. Greaves, *J. Solid State Chem.*, 1983, **49**, 325–333.

32 R. Grau-Crespo, A. Y. Al-Baitai, I. Saadoune and N. H. De Leeuw, *J. Phys.: Condens. Matter*, 2010, **22**, 255401.

33 C. Pecharromán, T. González-Carreño and J. E. Iglesias, *Phys. Chem. Miner.*, 1995, **22**, 21–29.

34 P. M. Woodward, E. Suard and P. Karen, *J. Am. Chem. Soc.*, 2003, **125**, 8889–8899.

35 L.-S. Zhong, J.-S. Hu, H.-P. Liang, A.-M. Cao, W.-G. Song and L.-J. Wan, *Adv. Mater.*, 2006, **18**, 2426–2431.

36 *Two-in-One Strategy for Effective Enrichment of Phosphopeptides Using Magnetic Mesoporous γ-Fe₂O₃ Nanocrystal Clusters*, ACS Applied Materials & Interfaces, 2020, https://pubs.acs.org/doi/abs/10.1021/am3019806.

37 S. Kamali, C. J. Chen, B. Bates, C. E. Johnson and R. K. Chiang, *J. Phys.: Condens. Matter*, 2020, **32**, 015302.

38 M. Tadic, S. Kralj and L. Kopanja, *Mater. Charact.*, 2019, **148**, 123–133.

39 T. Hyeon, S. S. Lee, J. Park, Y. Chung and H. B. Na, *J. Am. Chem. Soc.*, 2001, **123**, 12798–12801.

40 B. Zhang, Q. Wang, G. Zhang, S. Liao, Z. Wang and G. Li, *Plasma Sci. Technol.*, 2015, **17**, 876–880.

41 C. Rath, N. C. Mishra, S. Anand, R. P. Das, K. K. Sahu, C. Upadhyay and H. C. Verma, *Appl. Phys. Lett.*, 2000, **76**, 475–477.

42 Z. Nemati, J. Alonso, H. Khurshid, M. H. Phan and H. Srikanth, *RSC Adv.*, 2016, **6**, 38697–38702.

43 R. Naik, U. Senaratne, N. Powell, E. C. Buc, G. M. Tsoi, V. M. Naik, P. P. Vaishnava and L. E. Wenger, *J. Appl. Phys.*, 2005, **97**, 10J313.

44 S. Suresh, S. Karthikeyan and K. Jayamoorthy, *J. Adv. Res.*, 2016, **7**, 739–747.